A Poroelastic Model That Predicts Some Phenomenological Responses of Ligaments and Tendons

T. S. Atkinson

R. C. Haut

N. J. Altiero

Orthopaedic Biomechanics Laboratories,
College of Osteopathic Medicine, and
Department of Materials Science
and Mechanics,
College of Engineering,
Michigan State University,
East Lansing, MI 48824

Experimental evidence suggests that the tensile behavior of tendons and ligaments is in part a function of tissue hydration. The models currently available do not offer a means by which the hydration effects might be explicitly explored. To study these effects, a finite element model of a collagen sub-fascicle, a substructure of tendon and ligament, was formulated. The model was microstructurally based, and simulated oriented collagen fibrils with elastic-orthotropic continuum elements. Poroelastic elements were used to model the interfibrillar matrix. The collagen fiber morphology reflected in the model interacted with the interfibrillar matrix to produce behaviors similar to those seen in tendon and ligament during tensile, cyclic, and relaxation experiments conducted by others. Various states of hydration and permeability were parametrically investigated, demonstrating their influence on the tensile response of the model.

Introduction

Tendons and ligaments provide stability and control for the motion of joints. Thus, their function plays an important role in musculoskeletal biomechanics. Assessment of the mechanical properties of these tissues is important in development of various surgical techniques for joint reconstruction. In these assessments, the role of collagen fibers in the tissue has been highlighted and correlated to various disease states. Models that refer to various collagen morphologies have been used to characterize the results of these studies (Belkoff and Haut, 1992; Lanir, 1978; Kwan and Woo, 1989).

More recently, experimental studies have suggested that other tissue components, such as water (which comprises 60–70 percent of the weight of tendons and ligaments), might play a significant role in the tensile behavior of ligaments and tendons. For example, experiments suggest that human patellar tendons exhibit higher tensile modulus and ultimate strength when tested in a bath environment versus in air (Haut and Powlison, 1990). Similarly, the tendon is stiffer when tested in a hydrating solution versus a dehydrating solution (Haut et al., 1995). Furthermore, both studies suggest that the viscoelastic properties of human tendon are influenced by water. For example, in relaxation tests, specimens tested in a saline bath exhibit a larger and more rapid load relaxation versus those tested in air (Haut and Powlison, 1990). Similarly, specimens tested in a hydrating bath have greater load relaxation than those tested in a dehydrating bath (Haut et al., 1995).

In ligaments, increasing the water content causes the tissue to respond with greater cyclic load relaxation relative to ligaments with lower water content (Chimich et al., 1992). Data from cyclic tests also demonstrate monotonic decreases in rat tail tendon diameter from cycle to cycle (Lanir et al., 1988). Similar behavior has been documented in the rat medial collateral ligament (MCL) (Thielke et al., 1995). This deformation suggests densification of the collagenous structure and exudation of fluid, and is consistent with reports that glycosaminoglycans (GAGs) and water are exuded during tensile strain tests (Lanir et al., 1988; Hannafin and Arnoczky, 1994).

Effects associated with extracellular water have been observed experimentally, but few analytical models address the mechanism of its action. Chen et al. (1993) utilized a finite element analysis (FEA) to study permeability effects in tendon and ligament. The model includes a fluid phase moving around regular cylinders (meant to represent collagen fibers). Chen and Vanderby (1994) proposed a directionally sensitive permeability for tendons. The influence of water has also recently been incorporated in a model of the rabbit MCL (Wilson et al., 1994). Wilson's FEA model utilizes a continuum matrix of poroelastic material and spring elements attached at nodes to include the elastic stiffness of collagen. The model predicts that pressure within the MCL is negative during tensile deformation, implying that fluid flows into the structure. This result, however, is contrary to current experimental data indicating positive internal pressures (Chen et al., 1995) in rabbit patellar tendon during tensile stretch and fluid exudation in the canine flexor tendon, rabbit MCL, and rat tail tendon under tensile strain (Hannafin and Arnoczky, 1994; Thielke et al., 1995; Lanir et al., 1988).

These contrary results suggest that continuum characterizations alone of the tendon may not reflect mechanisms important to predicting the role of water in tensile load response. Lanir et al. (1988) describe the tendon on a microscopic scale as consisting of an arrangement of collagen fibrils embedded in a hydrophilic gel. While there is controversy in the literature concerning the hierarchical levels of collagen, it is generally accepted that fibrils are combined to form sub-fasciculi, fasciculi, and finally the whole structure (Danylchuk et al., 1978; Viidik, 1990; Yahia and Drouin, 1988). It has been proposed that the morphology of collagen fibrils can be complex, ranging from being helically wound about a sub-fascicular (termed fascicle by Yahia and Drouin, 1988) axis in the patellar tendon to both helical and planar waveforms in the anterior cruciate ligament (ACL). In the sub-fasciculi containing helically wound fibrils, the peripheral fibrils appear as undulated helices, while the central ones are normal helices (Yahia and Drouin, 1989). It has been previously suggested that the collagen in tendon and ligament interacts in such a way that it compresses the gelatinous matrix and creates a sensitivity to strain rate in the

Contributed by the Bioengineering Division for publication in the JOURNAL OF BIOMECHANICAL ENGINEERING. Manuscript received by the Bioengineering Division January 3, 1996; revised manuscript received December 21, 1996. Associate Technical Editor: P. A. Torzilli.

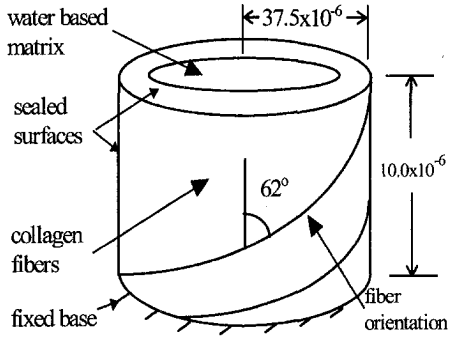

Fig. 1 Conceptualization of the geometry of a fascicle used as the basis of the finite element model

tissue (Lanir, 1978). We hypothesized that longitudinal deformation of the more helically oriented fibrils in the sub-fascicular structure of patellar tendons and ACLs might compress the matrix to generate hydraulic pressures and movement of unbound water during tensile stretch. By this mechanism the load might be shared between collagen and the surrounding matrix to influence the tensile response of the entire ligamentous or tendonous structure. Danylchuk et al. (1978) state that the connective tissue sheaths between fascicles and sub-fascicles contain collagen that is oriented perpendicular to the long axis of the structure and thus provides a binding function rather than significant tensile strength. We therefore assumed that the sub-fascicle may be considered a characteristic structure of ligament and tendon, which therefore should exhibit behaviors observed in the gross structure.

Methods

The fibril structure and matrix interaction were idealized for the purpose of building a simple model. This simple model consisted of an outer ring composed entirely of helically oriented fibrils, and an internal region comprised of a water-based matrix (Fig. 1). These regions interact to support tensile loads. Further simplifications of this conceptual model were made in order to provide the basis for a finite element model. The sub-fascicle's cross section was assumed to be circular and of constant diameter throughout its length. Thus, it was only necessary to model a representative section from the center of a centrally located sub-fascicle.

A finite element model, consisting of 84, 20-noded three-dimensional continuum elements, was developed using a commercial code (ABAQUS, Hibbitt, Karlsson, and Sorensen, Inc. Pawtucket R.I.). The cubic elements consisted of nodes at the midpoint of each edge possessing three degrees of freedom for displacement, and nodes at the corners possessing an additional degree of freedom for pressure. The model's radius, 37.5 μm, was an average of those scaled from micrographs of the human patellar tendon (Yahia and Drouin, 1988). The length of the model was chosen to be 10.0 μm to maintain an approximately one-to-one relationship between the lengths of the element sides in a majority of the elements and to help avoid numerical ill-conditioning. The fibrous outer ring was modeled as an orthotropic poroelastic material, where the selection of orthotropic material properties was intended to produce deformations consistent with helically oriented collagen fibrils. The fibril alignment, measured as a 62 deg inclination from vertical on one SEM of a tendon (Yahia and Drouin, 1988, Fig. 8), was attained by setting the 2 direction of the orthotropic outer ring at this inclination. For simplicity, the fibril morphology was assumed to be purely helical, at a constant angle of orientation through the sub-fascicle's thickness.

Little information is available documenting material properties of collagen sub-fascicles. One study suggests that rabbit patellar tendon fascicles have a modulus of approximately 225 MPa (Yamamoto et al., 1995). Rat tail tendon (RTT) has been described as being composed of one to three collagen fascicles (Kastelic et al., 1978) with a tensile modulus of approximately 600 MPa (Haut, 1983). In this study, the tensile modulus in the fibril direction was assumed to be 600 MPa (Table 1). Unfortunately, there is no information on the transverse or shear moduli of collagen sub-fascicles or fascicles. We assumed that the fibrous portion of the model was weak transverse to the fibril direction. Thus, the transverse moduli were assumed to be one order of magnitude less than the fibril direction modulus, and the shear moduli less than the transverse. Poisson ratios consistent with an orthotropic material were then selected.

The central core was modeled as nonlinear poroelastic. The poroelastic material model, originally developed to describe soil behavior, is similar in formulation to the biphasic model currently applied to cartilage (Suh and Spilker, 1994; Mow et al., 1984). The poroelastic matrix of tendon and ligaments may be similar to cartilage in that it is a fiber embedded permeable structure that contains water, proteoglycans, and other constituents (Mow and Hayes, 1991; Thielke et al., 1995).

The nonlinear poroelastic material stiffens upon compression. This is accomplished through moderation of the shear modulus in the following way:

$$G = \left[\frac{3(1-2\nu)(1+e_0)}{2(1+\nu)\kappa}\right](P + P_t)\exp(\epsilon_{\text{vol}}^{el})$$

where e_0 is the initial void ratio (volume fraction of fluid/volume fraction of solid), P is the internal pressure, P_t is the elastic ultimate strength, $\epsilon_{\text{vol}}^{el} = \ln J^{el}$ is the elastic portion of volume change, ν is Poisson ratio, and κ is the log bulk modulus (relating the logarithm of pressure to the dilatation) (Abaqus, 1972). Thus, G increases with compaction and pressure. Assuming that the volume fraction of water in tendon is similar to the weight fraction (70 percent of the wet weight is water), an initial void ratio of 2.33 (= 0.7/0.3) was used for the nonlinear poroelastic portion of the model (Haut, 1993; Mow and Hayes, 1991), however, e_0 = 1.0 (50 percent) was also investigated. Based on the assumption that fluid in tendon is similar to that in other tissues, the log bulk modulus of the nonlinear poroelastic core was obtained from data for fluid in the human annulus fibrosis (Best et al., 1989). The Poisson ratio was assumed to be 0.49. The tensile modulus of the material was then derived such that the initial shear modulus of the inner core approximately matched the shear moduli of the outer poroelastic ring.

Fluid flow was assumed to obey Darcy's law, i.e.,

$$v = -kdp/dr$$

where v is the fluid velocity, k is the permeability, and p is the pressure. This law is applicable to low flow rate problems and is used in biphasic models of cartilage (Mow and Hayes, 1991). The influence of permeability on flow rate can be complex and is known to be a nonlinear function of deformation in cartilage (Mow et al., 1984). Since k is unknown for tendon, it was assumed constant. In the past, similar assumptions have been utilized in cartilage models (Suh and Spilker, 1994). The permeability of cartilage has been reported from 1.45×10^{-15} (bovine) to 2.17×10^{-15} m^4/Ns (human patellar groove) (Mow and Hayes, 1991). Permeabilities in the range 1.0×10^{-12} to 1.45×10^{-27} m^4/Ns were investigated in the current study.

Table 1 Material coefficients

Elastic Moduli	Value	Poisson's Ratio	Value	Shear Moduli	Value
E1	30MPa	v12	.01	G1	.5 MPa
E2	600MPa	v23	.25	G2	.5 MPa
E3	30MPa	v13	.25	G3	.5 MPa

The orthotropic poroelastic material of the outer ring was assumed to be capable of holding water with permeabilities similar to those of the core portion of the model. Initial voids ratios of 1.0 and 2.33, similar to those used in the core, were assigned to this portion, but values as low as 0.01 were also examined. All the materials in the model were assumed to be fully saturated and the outer ring was assumed to be perfectly attached to the inner core.

Boundary Conditions

All loading was prescribed through displacement control. The bottom of the model was constrained to planar motion with four nodes separated by 90 deg constrained to radial motion. The top of the model was also constrained to planar motion (r and θ free). A uniform displacement was applied across the top of the model. The top and bottom were assumed to be sealed in order to represent conditions in a long thin fascicle at the center of a tendon. The outer boundary of the model was also sealed. This sealed boundary condition was dictated by the use of continuum elements in the ring portion of the model (rather than modeling discrete collagen fibers), which would experience a positive dilatation under tensile loading and thus tend to draw in water if a perfectly draining boundary condition were applied. This drawing in of water would compete with the movement of water from the core part of the model, thus obscuring effects the model was designed to study. The sealed boundary condition forced fluid to flow according to gradients developed as result of the applied stress and not as a function of a drainage pressure applied as a boundary condition.

Relaxation experiments, similar to those performed by Haut et al. (1995), were simulated with the model with an initial, suddenly applied, 3 percent strain followed by a 180 s period of constant deformation. Constant strain-rate tensile tests, also similar to those in Haut et al. (1995), were simulated using constant strain rates of 0.5 percent/s and 50 percent/s. Cyclic extension tests, similar to those performed by Chen et al. (1995), Chimich et al. (1992), and Hannafin and Arnoczky (1994), were simulated using a 0.5 cycle per second 4 percent strain triangular ramp.

Parametric studies were also performed during the simulated relaxation and constant strain rate tests in which moduli, permeability, and void ratio were varied in both the ring and core portions of the model.

Newton's method with backward time integration was utilized to solve the coupled flow and deformation equations simultaneously. Since pilot studies indicated that shear deformations exceeded 10 percent, nonlinear deformation terms were included in the analysis. Due to the unsymmetric nature of the coupled flow equations, the unsymmetric matrix solver was used in all solutions.

Results

Constant Deformation Relaxation. In the simulated relaxation experiments the model indicated an initially high reaction force, which slowly relaxed to a lower, steady-state level (Fig. 2(a)). The relaxation response was highly sensitive to permeability and water content. Increasing permeability caused the sub-fascicle to relax to the steady state response faster. If k was less than 1×10^{-19} m^4/Ns, the relaxation phenomenon was lost in the time frame of the current study (0–180 s). If it was greater than 1×10^{-16}, the initial peak in the force was lost. Increased initial water content, reflected by an increase in e_0, tended to increase the peak force, steady-state force, and the amount of relaxation. Higher percentages of relaxation resulted when the water content and voids ratio were the same throughout the sub-fascicle, rather than varied between the fibrous ring and the poroelastic core.

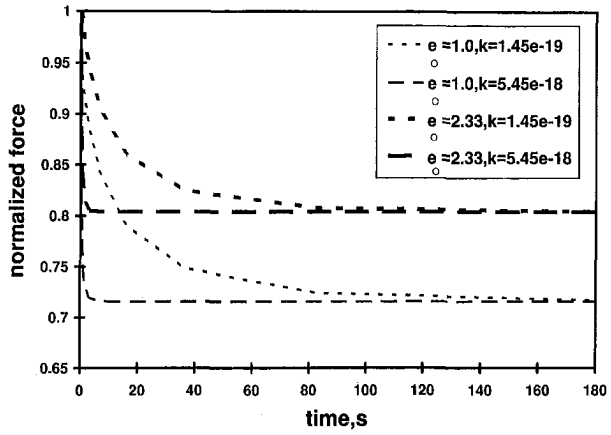

Fig. 2(a) The effects of void ratio and permeability on stress relaxation in a constant-deformation (3 percent strain) test. The forces were normalized by the peak force in the $e_0 = 2.33$, $k = 1.45 \times 10^{-19}$ m^4/Ns load case. For each load case, k and e_0 were constant throughout the model. The initial normalized force in the load cases $e_0 = 1$, $k = 1.45 \times 10^{-19}$ m^4/Ns, and 5.45×10^{-18} m^4/Ns was 0.95. The material constants for the outer ring are given in Table 1. The material constants in the poroelastic matrix were $\nu = 0.45$, $\kappa = 0.047$, and $P_t = 3.4 \times 10^5$ Pa.

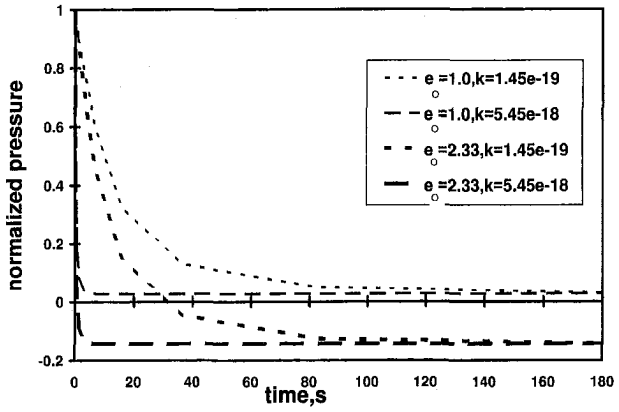

Fig. 2(b) The effects of void ratio and permeability on fascicle internal pressure during stress relaxation a constant deformation (3 percent strain) test. The pressures were normalized by the peak for in the $e_0 = 2.33$, $k = 1.45 \times 10^{-19}$ m^4/Ns load case.

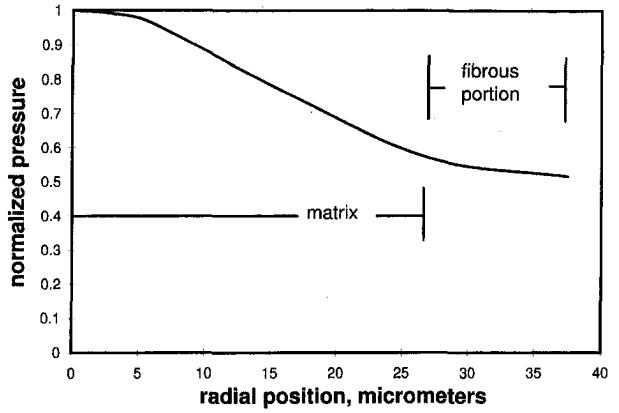

Fig. 2(c) Variation of pressure in the radial direction during the $e_0 = 1.0$ and $k = 1.45 \times 10^{-19}$ m^4/Ns load case

The internal pressures predicted during the constant deformation experiments also exhibited a dependence on water content and permeability. During this test the internal pressure within the sub-fascicle was initially high, but decreased to a lower steady-state value (Fig. 2(b)). Pressures central to the sub-fascicle were high, and decreased radially (Fig. 2(c)). The core portion of the model always experienced a negative dilatation.

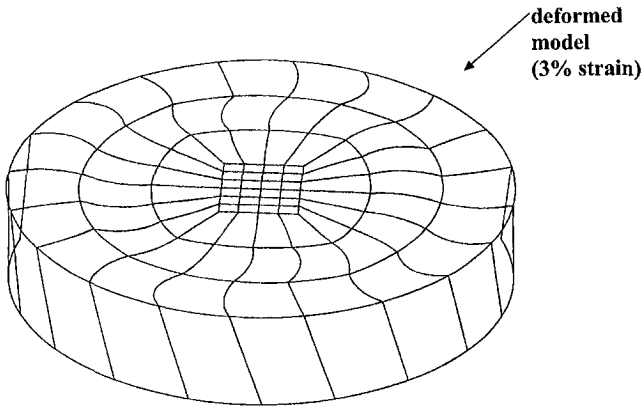

Fig. 3 Deformation of the model at 3 percent strain (magnified × 10) during a constant deformation test. The elements shear to the left, bringing the fiber axis (initially oriented at 62 deg to the right) more directly in line with the tensile load.

At steady state the pressures in the model were either positive, slightly negative, or close to zero, depending on the material properties selected. Combinations of properties that produced large negative pressures in the fibrous ring portion of the model resulted in negative steady-state pressures. Increasing e_0 increased the initial internal pressure. Increasing k increased the rate of pressure decay. Increased ultimate tensile strength of the poroelastic core, P_t, tended to decrease the peak pressure in the middle of the fascicle. The pressure at each location was constant through the model's length, and the initial pressure resulting in the fibrous ring was always negative.

The deformation of the ring elements was such that the fiber axis became more aligned with increasing axial load, causing the element to twist helically (Fig. 3). In addition, the radial deformation during these relaxation tests indicated that the sub-fascicle's radius decreased slightly as a function of time.

Cyclic Loading. During cyclic loading the sub-fascicle's internal pressures followed the applied loading (Fig. 4(a)). The peak internal pressures were positive, and the pressures when the displacement returned to zero were slightly negative. The peak pressures and axial force varied as a function of the extension, decreasing with increasing numbers of cycles. During the extension, the pressures at the center of the model were higher than those at the edge (Fig. 4(b)).

Tensile Deformation at Varied Rates. During simulated constant strain rate experiments, the sub-fascicle stiffness was dependent on initial water content, as defined by e_0. As the initial water content was increased, the model's stiffness increased (Fig. 5(a)). The sub-fascicle's stiffness was also dependent on the values chosen for k. Increasing k caused the stiffness to decrease for $1 \times 10^{-12} < k < 1 \times 10^{-15}$ m^4/Ns. At low permeability, there was no difference in stiffness due to changes in e_0. Increasing the various elastic moduli caused the model's stiffness to increase accordingly.

The model's stiffness was dependent on strain rate if $k > 1 \times 10^{-14}$ m^4/Ns (Fig. 5(b)). Faster rates of extension produced a stiffer response. Increasing P_t, or the transverse elastic moduli in the fibrous ring portion, or decreasing the permeability in any part of the model, decreased the sensitivity of stiffness to strain rate.

The force/deformation response of the model was linear for small strains.

Discussion

Many of the model's predicted relaxation behaviors were consistent with experimentally observed tendon and ligament data. The peak force, rate of relaxation, and relaxed force exhibited by the model depended on e_0, the initial ratio of water to substrate. When the amount of water in the sub-fascicle decreased, the initial force, steady-state force, and the rate of relaxation decreased. This caused the reduced relaxation modulus (slope of the normalized force, logarithm time curve) to decrease. This behavior is consistent with the observations of Haut et al. (1995) and exhibits the same time-varying character as that noted by Lanir et al. (1988) and Chimich et al. (1992). The peak force and rate of relaxation shown in the model also depended on k. Parametric studies demonstrated that the ability of the elastic part of the model to take on water was primarily governed by the permeability parameter. In the current model the core portion exhibited dilatation and water flow behaviors hypothesized to exist in the matrix of a sub-fascicle. The ring portion loaded the matrix in a twisting manner, which we hypothesize is similar to the effect produced by collagen fibrils within the sub-fascicle. In this model the ring also acted as a sink for water. Water moved out of the nonlinear poroelastic core material into the ring portion of the model similar to how we hypothesize it would move out of the real sub-fascicle, and ultimately out of the entire structure. Water motion out of tissues has been observed experimentally (Chimich et al., 1992; Lanir et al., 1988; Hannafin and Arnoczky, 1994). The water motion phenomenon in the model was readily seen in the simulated relaxation, where water initially trapped in the compressed poroelastic core of the model diffused out into the fibrous ring portion, thus softening the poroelastic portion and decreasing the overall tensile stress.

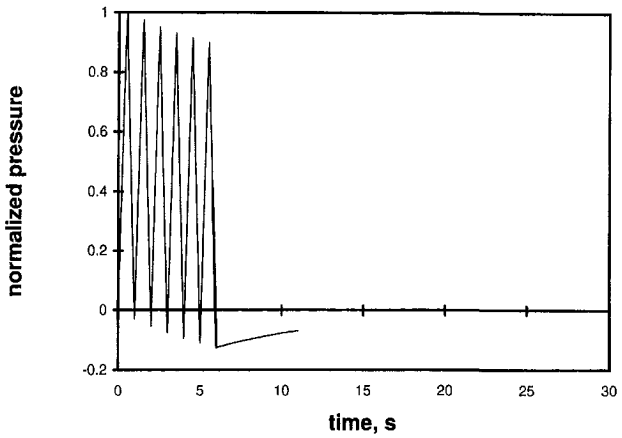

Fig. 4(a) Fascicle internal pressures during cyclic deformation. Pressures were normalized by the peak positive pressure. Orthotropic material properties are given in Table 1, e_0 = 0.01, and $k = 1.45 \times 10^{-19}$ m^4/Ns. Poroelastic properties were e_0 = 1.0, $k = 1.45 \times 10^{-14}$ m^4/Ns, ν = 0.49, $P_t = 3.4 \times 10^4$ Pa, and κ = 0.047.

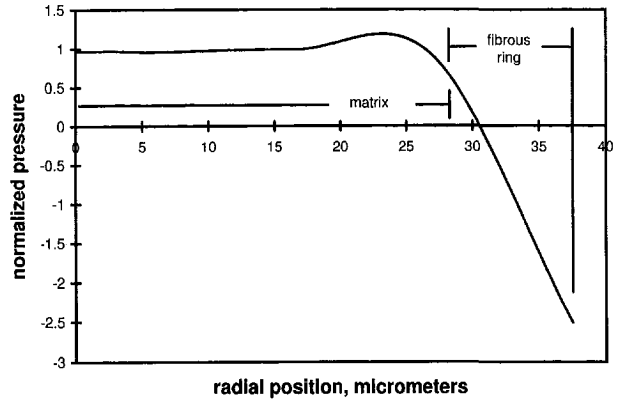

Fig. 4(b) Fascicle pressures as a function of radial distance at the peak of the first cycle

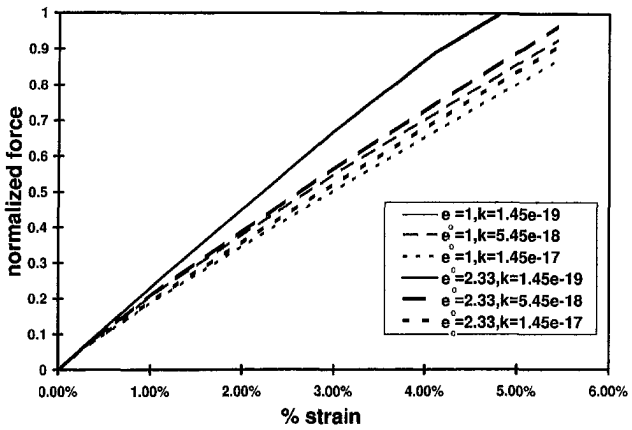

Fig. 5(*a*) The effect of void ratio and permeability during constant strain rate tensile deformation (10 percent/s). Forces were normalized by the force at 4.8 percent strain in the $e_0 = 2.33$, $k = 1.45 \times 10^{-19}$ m^4/Ns load case. The lines for the load cases $e_0 = 1$, $k = 1.45 \times 10^{-19}$ m^4/Ns and $e_0 = 2.33$, $k = 1.45 \times 10^{-19}$ m^4/Ns are on top of one another. The material constants in the ring portion of the model are given in Table 1. The material constants in the poroelastic matrix were $\nu = 0.45$, $\kappa = 0.047$, and $P_t = 3.4 \times 10^4$ Pa.

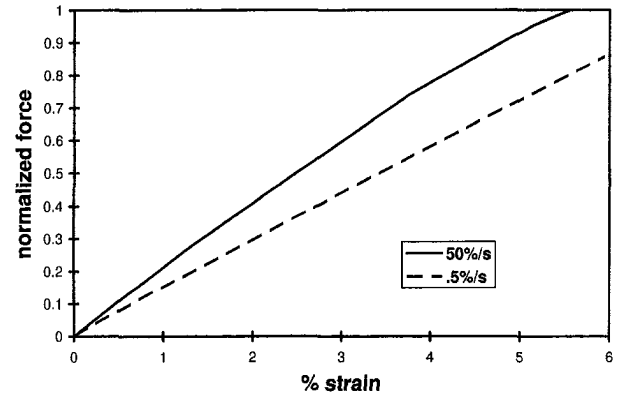

Fig. 5(*b*) The effect of strain rate on the tensile response of the fascicle. For both tests $e_0 = 2.33$ and $k = 1.45 \times 10^{-17}$ m^4/Ns. The material constants in the ring portion of the model are given in Table 1. The material constants in the poroelastic matrix were $\nu = 0.45$, $\kappa = 0.047$, and $p_t = 3.4 \times 10^4$ Pa.

The model's pressure profile was also similar to that in a recently reported experiment, which indicated that the internal pressure developed in a rabbit patellar tendon during cyclic loading is positive and follows the loading profile (Chen et al., 1995). The model also predicted a concurrent decrease in the diameter of the sub-fascicle during the test. This phenomenon was consistent with experimental observations in rat tail tendon (Lanir et al., 1988) and in rat MCL (Thielke et al., 1995). It has been suggested that this decreasing cross-sectional area indicates compaction and water motion out of the interfibrillar matrix (Hannafin and Arnoczky, 1994; Lanir et al., 1988; Thielke et al., 1995). These phenomena are consistent with observations made in the current parametric studies using the poroelastic model.

During cyclic extension, the model's internal pressures were positive on extension, negative on the return to zero displacement, and the peak pressures and forces decreased with increasing number of cycles. This behavior was similar to the experimental pressure measurements of Chen et al. (1995) in the rabbit patellar tendon. This pressure pattern was also consistent with water motion radially out of the poroelastic portion (into the elastic portion) during extension and back in when the displacement returned to zero. These predictions suggest that fluids tend to leave the sub-fascicle during cyclic loading, consistent with recent experimental findings (Hannafin and Arnoczky, 1994; Lanir et al., 1988). The predicted relaxation during cyclic loading was similar to that observed in ligaments (Chimich et al., 1992).

In the experiment of Chen et al. (1995), the magnitude of the measured pressure was significantly less than the tensile stress, suggesting a lack of load sharing between the fibers and matrix. In the current study, cyclic loading tests showed that the peak predicted pressures in the matrix portion of the sub-fascicle were similar to the average stress (average force/area). Thus, the current model suggested there was load sharing. It is possible that Chen's pressure probe provided a leakage path for water. On the other hand, the model describes a very small unit of the tendon and predicted pressures might not reflect gross pressures measured in the tendon. This difference might also be attributed to possible differences in the water content of rabbit patellar tendon and human tendon. As the pressures predicted in the model also depend on the void ratio and permeability, additional parameter studies performed under cyclic loading may provide more insight into these experimentally observed behaviors.

In simulated constant-rate-of-deformation tensile tests (10 percent/s), the sub-fascicle's stiffness increased when the void ratio (water fraction) increased. Similar behavior has been noted in tendons when the test environment was used to alter the water content (Haut and Powlison, 1990; Haut et al., 1995). This behavior resulted in the model when the void ratio was increased in either both the elastic and poroelastic parts or just in the poroelastic part. Variation of the initial amount of water in the elastic part does not in itself change the stiffness of the elastic portion. However, anything that alters the ability of the elastic portion to accept water from the poroelastic portion affected the stiffness of the poroelastic portion and thus the stiffness of the total model. The sub-fascicle stiffness also exhibited a dependence on permeability. Increasing the permeability tended to make the model more compliant. Although no direct evidence exists documenting the permeability of tendons, previously Haut and Powlison attributed the increased compliance of γ-irradiated tendons to increased permeability. At lower permeability, changes in the voids ratio did not affect the sub-fascicle stiffness. This suggests that the water acts as a stiffening agent only when the permeability of the tendon is sufficiently high. The force–deformation curve provided by the model was linear, unlike the force-deformation curves for a gross tendon or groups of fascicles (Butler et al., 1986). This discrepancy is attributed to the simplified fibril morphology incorporated in the model. Factors such as variation of fibril orientation through the sub-fascicle thickness, the undulation of fibrils, sub-fascicle recruitment, and sub-fascicle interactions were not examined in the current study, but should be addressed in future models.

When the rate of deformation was changed from 10 percent/s to other rates of extension, the model exhibited rate sensitivity. During fast extension (50 percent/s) the model predicted a stiffer response than that during slow extension (0.5 percent/s), similar to Haut et al. (1995). This behavior was highly dependent on the tissue permeability, with no rate dependence exhibited at $k < 1 \times 10^{-14}$ m^4/Ns. This suggests that the water motion in the tissue might cause rate sensitivity when the permeability of the tendon is sufficiently high.

Deformation in the model's outer ring was consistent with collagen fibrils reorienting into a tighter, more axially aligned helix. This deformation produced a wringing effect in the sub-fascicle, compressing the hydrophilic gel portion to generate positive pressure. This particular deformation may then be very important in producing many of the observed mechanical behaviors particular to tendons and ligaments.

Although the model exhibits behaviors consistent with many experimentally observed behaviors, several problems remain that must be addressed in its further development. The distribution and morphology of collagen fibrils in the sub-fascicle have been simulated by the use of a fibrous ring attached to the

outside of the core, matrix material. As the ring material is somewhat compressible, it experienced a positive dilatation under tensile load leading to negative negative pressures in the ring. Yet, on the other hand, the model exhibited a wringing out of the core and thus water motion out of the sub-fascicle. We hypothesize that water flow effects exhibited by the core of our model will occur throughout a real sub-fascicle as real fibrils experience rigid body motion motion as they align along the loading axis. Improvements such as distributing elements throughout the matrix to represent fibrils might lead to a more realistic microstructural model of the sub-fascicle. Another limitation of the current model is that the thin connective tissue sheaths that separate sub-fascicles have not been included in the model. However, we hypothesize that these thin sheaths do not play an active role in the tensile response of tendon and ligament; rather, they act to bind sub-fascicles and fascicles into the gross structure. The model's tensile response was compared qualitatively to that of whole tendon or ligament; however, interactions between sub-fascicles and extra-fascicular materials must be evaluated experimentally before a whole tendon model can be developed. Strategies to utilize the model to describe whole tendon and ligament behavior quantitatively remain to be explored. Appropriate material properties must also be obtained. The bulk modulus (κ) of the interstitial fluid, the fascicle's elastic modulus, the angle of fibril orientation, and other geometric properties need to be measured. Other material properties, such as the transverse elastic moduli and the shear moduli, might be assumed, or could be derived based on SEM studies of fibril reorientation during tensile loading with the use of this analytical model. The model also suggests that parameters such as the tissue permeability (k) and void ratio (e_0) are extremely important. These parameters might be measured using standard permeability tests and measurements of water content.

The model demonstrates that when structural aspects, i.e., collagen morphology and orientation, and aspects of how collagen interacts with the hydrophilic base matrix material, are taken into account, a reasonable mechanical response results. The sub-fascicle modeled here is similar in form to those found in both the patellar tendon and ACL. Other fascicle morphologies also exist in the ACL and require further study, but the approach taken in modeling this structure may serve as a basis for such a model. We suggest that future improvements in the understanding of ligament and tendon mechanics will necessarily involve the study of microstructure and the measurement of parameters not previously considered. Thus, we propose that analytical models that incorporate tissue water content and microstructural information will be important tools in future research.

References

Abaqus, 1994, "Theory Manual," Version 5.4, Hibbitt, Karlsson, and Sorenson, Inc., pp. 4.4.1.

Belkoff, S. M., and Haut, R. C., 1992, "Microstructurally based model analysis of γ-irradiated tendon allografts," *J. Othop. Res.,* Vol. 10, pp. 461–464.

Best, B. A., Setton, L. A., Guilak, A., Ratcliffe, A., Weidenbaum, M., and Mow, V. C., 1989, "Permeability and compressive stiffness of annulus fibrosus: variation with site and composition," *Trans. Orthop. Res. Soc.,* Vol. 14, p. 354.

Butler, D. L., Matthew, D. K., and Donald, C. S., 1986, "Comparison of material properties in fascicle-bone units from human patellar tendon and knee ligaments," *J. Biomech.,* Vol. 19, No. 6, pp. 425–432.

Chen, C., McCabe, R., and Vanderby, R. Jr., 1995, "Two electrokinetic phenomena in rabbit patellar tendon: pressure and voltage," *Proc. ASME Bioengineering Conf.,* Beaver Creek, CO, pp. 31–32.

Chen, C. T., Vanderby, R., Graf, B. K., and Malkus, D. S., 1993, "Interstitial fluid flow in ligaments and tendons: effects of fibril spacing and fluid properties," *Proc. ASME Bioengineering Conf.,* Breckenridge, CO, pp. 399–402.

Chen, C. T., and Vanderby, R., 1994, "3-D finite element analysis to investigate anisotropic permeability for interstitial fluid flow in ligaments and tendons," *Trans. Orthop. Res. Soc.,* Vol. 19, p. 643.

Chimich, D. D., Shrive, N. G., Frank, C. B., Marchuk, L., and Bray, R. C., 1992, "Water content alters viscoelastic behaviour of the normal adolescent rabbit medial collateral ligament," *J. Biomech.,* Vol. 25(8), pp. 831–837.

Danylchuk, K. D., Finlay, J. B., and Krcek, J. P., 1978, "Microstructural organization of human and bovine cruciate ligaments," *Clinical Orthopaedics and Related Research,* No. 131, pp. 294–298.

Hannafin, J. A., and Arnoczky, S. P., 1994, "Effect of cyclic and static tensile loading on the water content and solute diffusion in canine flexor tendons: an in-vitro study," *J. Orthop. Res.,* Vol. 12, pp. 350–356.

Haut, R. C., 1983, "Correlation between strain-rate-sensitivity in rat tail tendon and tissue glycosaminoglycans," *Proc. ASME Biomechanics Symposium,* pp. 221–224.

Haut, R. C., and Powlison, A. C., 1990, "The effects of test environment and cyclic stretching on the failure properties of human patella tendons," *J. Orthop. Res.,* Vol. 8, pp. 532–540.

Haut, R. C., 1993, "The mechanical and viscoelastic properties of the anterior cruciate ligament and of ACL fascicles," in: *The Anterior Cruciate Ligament: Current and Future Concepts,* Jackson, D. W., et al., eds., Raven Press, Ltd., New York.

Haut, T. L., Jayaraman, R. C., and Haut, R. C., 1995, "Water content determines the strain rate sensitive stiffness of human patellar tendon," *Advances in Bioengineering,* ASME BED-Vol 31, pp. 61–62.

Kastelic, J., Galeski, A., and Baer, E., 1978, "The multicomposite structure of tendon," *Connective Tissue Res.,* Vol. 6, pp. 11–23.

Kwan, M. K., and Woo, S. L.-Y., 1989, "A structural model to describe the nonlinear stress-strain behavior for parallel-fibered collagenous tissues," ASME JOURNAL OF BIOMECHANICAL ENGINEERING, Vol. 111, pp. 361–363.

Laible, J. P., Pflaster, D., Simon, B. R., Krag, M. H., Pope, M., and Haugh, L. D., 1994, "A dynamic material parameter estimation procedure for soft tissue using a poroelastic finite element model," ASME JOURNAL OF BIOMECHANICAL ENGINEERING, Vol. 116(1), pp. 19–29.

Lanir, Y., 1978, "Structure–strength relations in mammalian tendon," *Biophysical J.,* Vol. 24, pp. 541–554.

Lanir, Y., Saland, E. L., and Foux, A., 1988, "Physico-chemical and microstructural changes in collagen fiber bundles following stretch in-vitro," *Biorheology J.,* Vol. 25(4), pp. 591–604.

Mow, V. C., Holmes, M. H., and Lai, W. M., 1984, "Fluid transport and mechanical properties of articular cartilage: a review," *J. Biomech.,* Vol. 17(5), pp. 377–394.

Mow, V. C., and Hayes, W. C., 1991, *Basic Orthopaedic Biomechanics,* Raven Press, Ltd., New York, pp. 143–243.

Simbeya, K. W., Shrive, N. G., Frank, C. B., and Matyas, J. R., 1993, "A micro-mechanical finite element model of the rabbit medial collateral ligament," *Recent Advances in Computer Methods in Biomechanics and Biomedical Engineering,* Middleton, J., Pande, G., and Williams, K., eds., Books and Journals Ltd., Swansea, pp. 240–249.

Suh, J., and Spilker, R. L., 1994, "Indentation analysis of biphasic articular cartilage: nonlinear phenomena under finite deformation," ASME JOURNAL OF BIOMECHANICAL ENGINEERING, Vol. 116, pp. 1–9.

Thielke, R. J., Vanderby, R., Jr., and Grood, E. S., 1995, "Volumetric changes in ligaments under tension," *Proc. ASME Bioengineering Conf.,* Breckenridge, CO, pp. 197–198.

Viidik, A., 1990, "Structure and function of normal and healing tendons and ligaments," in: *Biomechanics of Diarthrodial Joints Vol I,* Mow, V. C., Ratcliffe, A., and Woo, S. L.-Y., eds. Springer-Verlag, New York, p. 3–12.

Wilson, A. N., Frank, C. B., and Shrive, N. G., 1994, "The behaviour of water in the rabbit medial collateral ligament," *Proc. Second World Congress of Biomechanics,* Blankevoort, L., and Kooloos, J. G. M., eds., Amsterdam, The Netherlands, p. 226b.

Yahia, L. H., and Drouin, G., 1988, "Collagen structure in human anterior cruciate ligament and patellar tendon," *J. Mat. Sci.,* Vol. 23, pp. 3750–3755.

Yahia, L. H., and Drouin, G., 1989, "Microscopical investigation of canine anterior cruciate ligament and patellar tendon: collagen fascicle morphology and architecture," *J. Orthop. Res.,* Vol. 7, pp. 243–251.

Yamamoto, E., Kozaburo, H., and Yamamoto, N., 1995, "Mechanical properties of collagen fascicles of stress-shielded patellar tendons in the rabbit," *Proc. Bioengineering Conf.,* Beaver Creek, CO, pp. 199–200.

Zienkiewicz, O. C., and Naylor, D. J., 1972, "The adaptation of critical state solid mechanics theory for use in finite elements," in: *Stress-Strain Behavior of Soils,* Parry, R. H. G., ed., Foulis and Co, pp. 537–543.